Journal of Polymer Research (2006) 13: 237–245
DOI: 10.1007/s10965-005-9031-9


# Synthesis and Opto-electrical Properties of Stellar Polyfluorene Derivatives Containing Polyhedral Oligomeric Silsesquioxanes as the Center Core

Kuei-Bai Chen, Hung-Yi Chen, Sheng-Hsiung Yang and Chain-Shu Hsu*
*Department of Applied Chemistry, National Chiao Tung University, 1001, Ta-Hsueh Rd., Hsinchu, 30010 Taiwan, Republic of China*
*(*Author for correspondence; Tel.: +886-3-5131523; Fax: +886-3-5131523; E-mail: cshsu@mail.nctu.edu.tw)*

Received 28 July 2005; accepted in revised form 2 November 2005

*Key words:* keto effect, polyfluorene, silsesquioxanes

**Abstract**

Three polyfluorene derivatives (**P1**–**P3**) emitting blue, green and red light were prepared via a Suzuki coupling method. Polyhedral oligomeric silsesquioxanes (POSS) were integrated into the center core of the derivatives to create stellar light-emitting polymers (**POSS-P1**–**POSS-P3**). The glass-transition and decomposition temperatures were raised after introducing POSS moieties. The starlike polymers showed a reduced emissive band at 540 nm when annealing at 200 °C. The result implies that integrated POSS at the center core suppresses the keto effect generally occurring for polyfluorenes. Double-layer light-emitting devices of indium tin oxide/poly(ethylenedioxythiophene)/polymer/Ca/Al were fabricated to evaluate polymer potential. Compared with pristine polymers, the maximum brightness and the current efficiency of devices using POSS-containing polymers as active layers were enhanced. A blending method using **P1** or **POSS-P1** as the host matrix further improved device performance.

## Introduction

Since the first report on polymer light-emitting diodes [1], a number of $\pi$-conjugated polymers have been intensively investigated in order to fabricate devices for industrial applications [2–4]. Poly(*p*-phenylene vinylene) has been widely used in recent years owing to its particular structure and highly electroluminescent properties [5]. However, pure blue and red emissive colors are difficult to achieve with PPV derivatives. Polythiophene derivatives show a wide emission from the blue to red region, yet the luminescence and efficiency are not elevated. Polyfluorene (PF) has been studied extensively of late because of its blue emission. The versatility of the emissive light obtained by copolymerizing PFs with different chromophores makes PFs good candidates for light-emitting applications [6–8]. The liquid-crystalline nature of most PFs can also be practically applied to polarized light emission [9].

Although PFs serve as excellent materials for light-emitting applications, the so-called keto effect occurs with alkyl chains at the C-9 position [10, 11]. The keto defect sites form at high temperatures or during long-term operation. The formation of fluorenone produces an additional emission band at longer wavelengths and changes the emissive color of the original PF. The aggregate/excimer formation also reduces device performance. Several modifications were proposed to reduce aggregation and the keto effect. The introduction of a spiro structure at the C-9 position is an effective design to suppress keto defects [12]. Recently polyhedral oligomeric silsesquioxanes (POSS) were incorporated into PFs to reduce aggregation as well as to enhance thermal stability [13–15].

In this study, three PF derivatives emitting blue, green and red light were synthesized. Incorporation of POSS into the center core links PFs, causing them to form starlike polymers. The synthesized materials were used as active layers in double-layer devices to evaluate their electro-optical properties. Finally, the blending method was also applied to further enhance the device performance.

## Experimental

### *Characterization methods*

$^1$H-NMR spectra were measured with a Varian 300-MHz spectrometer. Gel permeation chromatography data assembled from a Viscotek T50A differential viscometer and an LR125 laser refractometer and three columns in series were used to measure the molecular weights of polymers relative to polystyrene standards at 35 °C. IR spectra were obtained by using a PerkinElmer Spectrum One spectrophotometer in the range 400–4,000 cm$^{-1}$. Wide-angle X-ray diffraction was performed with a BEDE D1 instrument. Differential scanning calorimetry (DSC) was performed using a PerkinElmer Pyris Diamond DSC instrument at a heating rate of 10 °C min$^{-1}$ and a cooling rate of 50 °C

$min^{-1}$. Thermal gravimetric analysis (TGA) was undertaken with a PerkinElmer Pyris 1 TGA instrument with a heating rate of 10 °C $min^{-1}$. UV–vis absorption spectra were obtained with an HP 8453 diode-array spectrophotometer. Photoluminescence (PL) emission spectra were obtained using an ARC SpectraPro-150 luminescence spectrometer. Cyclic voltammetric measurements were made with an Autolab ADC 164 instrument in acetonitrile with 0.1 M tetrabutylammonium hexafluorophosphate as the supporting electrolyte at a scan rate of 50 mV $s^{-1}$. Platinum wires were used as both the counter electrode and the working electrode, and silver/silver ions (Ag in 0.1 M $AgNO_3$ solution, from Bioanalytical Systems.) was used as the reference electrode. Ferrocene was used as an internal standard, and the potential values were obtained and converted to values vs the saturated calomel electrode. The corresponding highest occupied molecular orbital (HOMO) and lowest unoccupied molecular orbital energy levels were estimated from the onset redox potentials.

### *Synthesis of monomers M1–M6*

All reagents and chemicals were purchased from commercial sources (Aldrich, Lancaster or TCI) and were used without further purification. Tetrahydrofuran (THF) and toluene were dried by distillation from sodium/benzophenone and calcium hydride, respectively. Scheme 1 outlines the synthesis of monomer **M3**. The detailed syntheses of monomers **M1**, **M2** and **M4**–**M6** were described previously [16–18].

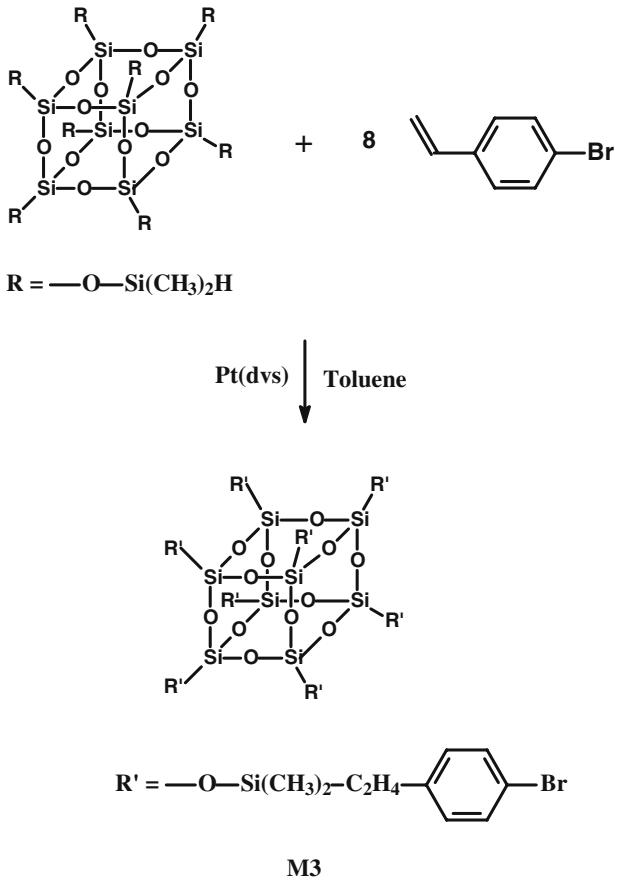


*Scheme 1.* Synthesis of monomer **M3**.

### *Octa[2-(4-Bromophenyl)enthyl]octakis(dimethylsilyloxyl) silsequioxane (M3)*

To a mixture of octakis(dimethylsilyloxyl)silsequioxane (0.5 g, 0.5 mmol) and 4-bromostyrene (0.8 g, 4.3 mmol) were added 10 drops of 1 wt% platinum divinyltetramethyldisiloxane [Pt(dvs)] and 10 mL of anhydrous toluene. The mixture was then stirred at 50 °C for 24 h. After the reaction was completed, a small amount of active carbon was added to adsorb Pt(dvs) and the solution was filtered with celite. The filtrate was extracted with chloroform and concentrated in vacuo. The crude product was purified by gel chromatography on silica gel using 1:1 hexane/ethyl acetate as the eluent to give 1.01 g (81%) transparent liquid. $^1$H-NMR ($CDCl_3$, $\delta$, ppm): 0.25 (s, 48H, Si–$CH_3$), 0.286 (t, 9H, Si–$CH_2$–$CH_2$, $\beta$-adduct), 1.23–1.31 (m, 10.5H, –Si–CH–$CH_3$, $\alpha$-adduct), 2.15–2.2 (m, 3.5H, Si–$CH$–$CH_3$, $\alpha$-adduct), 2.57 (t, 9H, Si–$CH_2$–$CH_2$, $\beta$-adduct), 6.89–6.96 (m, 16H, aromatic H), 7.23–7.29 (m, 16H, aromatic H).

### *Synthesis of polymers POSS-P1–POSS-P3: general procedure*

Scheme 2 outlines the syntheses of the starlike materials **POSS1-P1**, **POSS-P2** and **POSS-P3**. An experimental procedure for the **POSS-P1** is given in the following. To a mixture of **M1** (0.25 g, 0.5 mmol), **M2** (0.5 g, 0.85 mmol), **M4** (0.16 g, 0.34 mmol), $Pd(PPh_3)_4$ (0.01 g, $8.6 \times 10^{-3}$ mmol), $K_2CO_3$ (0.55 g, 3.98 mmol) and Aliquat 336 (0.08 g, 0.2 mmol) were added 10 mL of anhydrous toluene and 2 mL of deionized water. The resulting mixture was refluxed at 85 °C for 5 days under a nitrogen atmosphere. **M3** ($1.74 \times 10^{-2}$ g. $6.8 \times 10^{-3}$ mmol) was then added and refluxed at the same temperature for 48 h. 4,4,5,5-Tetramethyl-1,3,2-dioxaborolane-2-ylbenzene (0.17 g, 0.85 mmol) was then added as an end-capping agent and refluxed at 70 °C for 24 h. The polymer was obtained by pouring the mixture into methanol and the mixture was filtered. the polymer was purified by dissolving it in THF and reprecipitating it from methanol twice. After drying under vacuum for 24 h, the polymer was obtained as a light-green solid (0.45 g, 55%).

**POSS-P1** $^1$H-NMR (300 MHz, $CDCl_3$, $\delta$, ppm): 7.82–7.41, 7.18–7.26 (m, 18H, aromatic *H*), 2.54 [t, 2H, Ph–$CH_2$–$(CH_2)_3$–$CH_3$], 1.88 [t, 4H, fluorene–$CH_2$–$(CH_2)_4$–$CH_3$], 1.60–0.78 (m, 31H, alkyl *H*).

**POSS-P2** $^1$H-NMR (300 MHz, $CDCl_3$, $\delta$, ppm): 8.01–7.66 (m, 8H, aromatic–*H*), 1.86 [t, 4H, fluorene–$CH_2$–$(CH_2)_4$–$CH_3$], 1.41–0.77 (m, 22H, alkyl *H*).

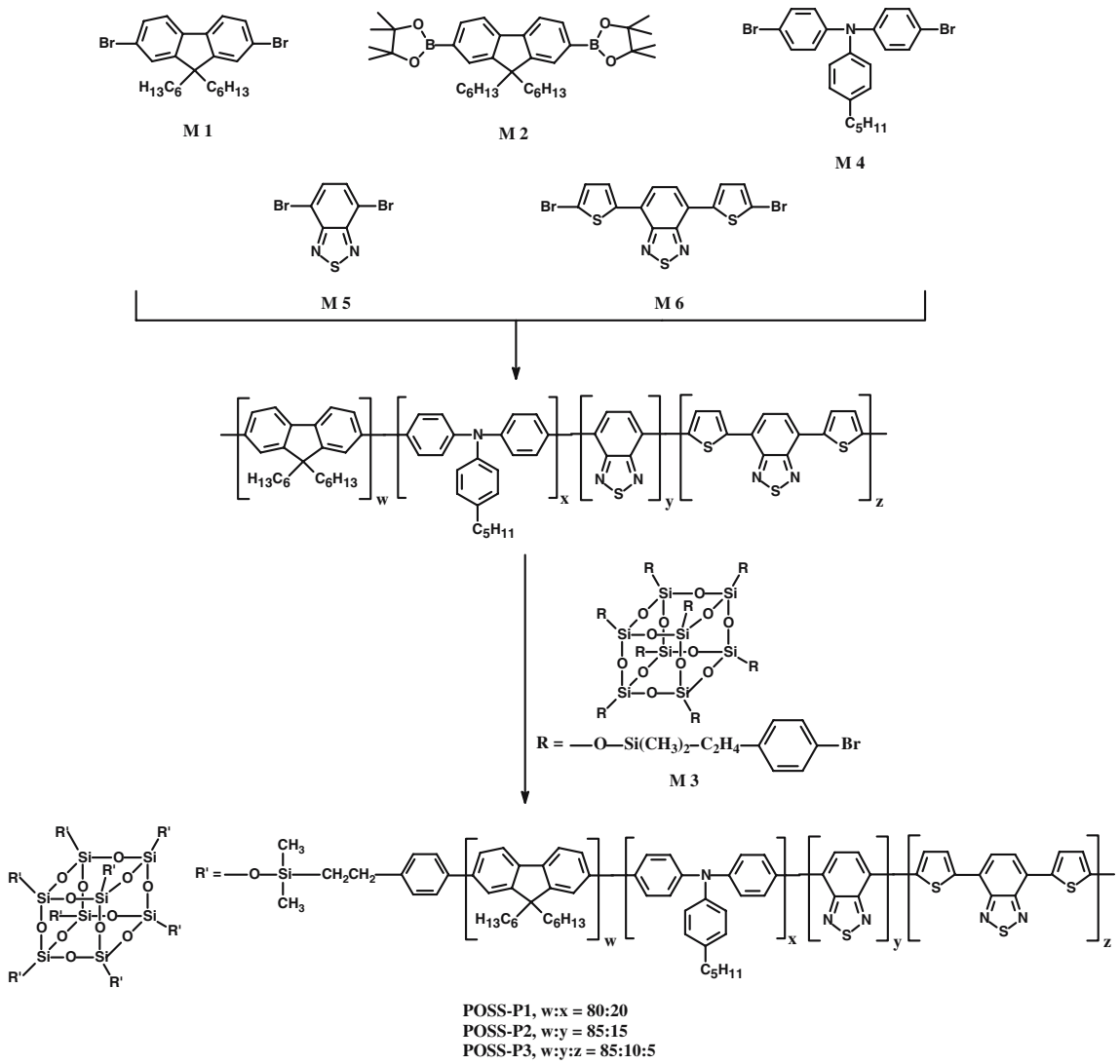


*Scheme 2.* Synthesis of polymers **P1**–**P3** and **POSS-P1**–**POSS-P3**.

**POSS-P3** $^1$H-NMR (300 MHz, $CDCl_3$, $\delta$, ppm): 7.84–7.66 (m, 14H, aromatic–*H*), 1.87 [t, 4H, fluorene–$CH_2$–$(CH_2)_4$–$CH_3$], 1.36–0.75 (m, 22H, alkyl protons).

*Device fabrication and measurements*

Double-layer devices were fabricated as sandwich structures between calcium cathodes and indium tin oxide (ITO) anodes. ITO-coated glass substrates were cleaned sequentially in ultrasonic baths of detergent, a 2-propanol/deionized water (1:1 volume) mixture, toluene, deionized water and acetone. A 50-nm-thick hole injection layer of poly(ethylenedioxythiophene) (PEDOT) doped with poly (styrenesulfonate) (PSS) was spin-coated on top of ITO from a 0.7 wt% dispersion in water and was dried at 150 °C for 1 h in a vacuum. Thin films of synthesized polymers were spin-coated from toluene solutions onto the PEDOT layer and dried at 50 °C overnight in a vacuum. The thickness of the active layer was approximately 50 nm. Finally, 35-nm Ca and 100-nm Al electrodes were made

*Table 1.* Composition ratio and polymerization results of polymers **P1**–**P3** and **POSS-P1**–**POSS-P3**

| Polymer | *w* | *x* | *y* | *z* | $\overline{M_n}(\times 10^{-3})$ | $\overline{M_w}(\times 10^{-3})$ | Polydispersity index | No. of arms |
|---|---|---|---|---|---|---|---|---|
| **P1** | 80 | 20 | | | 4.54 | 7.21 | 1.58 | |
| **POSS-P1** | 80 | 20 | | | 25.9 | 95.7 | 3.69 | 5.7 |
| **P2** | 85 | | 15 | | 7.97 | 14.0 | 1.87 | |
| **POSS-P2** | 85 | | 15 | | 28.6 | 84.9 | 2.96 | 3.5 |
| **P3** | 85 | | 10 | 5 | 9.87 | 20.9 | 2.12 | |
| **POSS-P3** | 85 | | 10 | 5 | 30.6 | 97.9 | 3.2 | 3.1 |

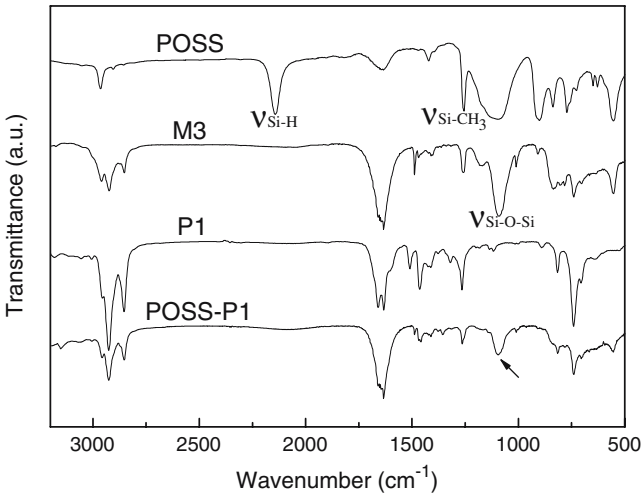


*Figure 1.* Fourier transform (*FT*) IR spectra of **POSS**, **M3**, **P1** and **POSS-P1**.

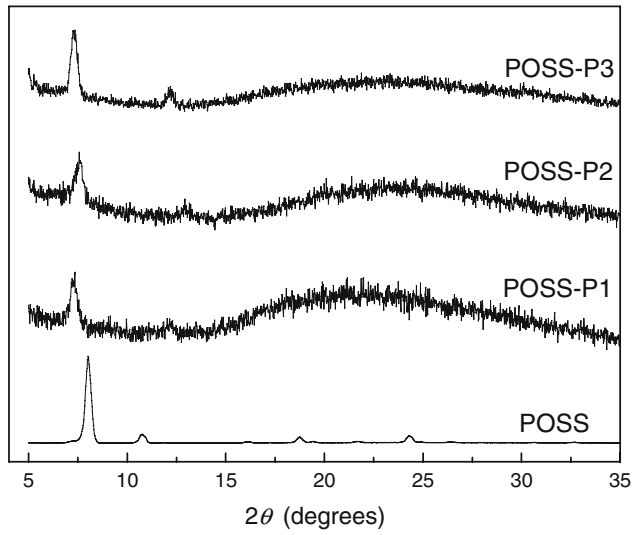


*Figure 2.* X-ray diffraction curves of **POSS** and **POSS-P1**–**POSS-P3**.

through a shadow mask onto the polymer films by thermal evaporation using an AUTO 306 vacuum coater (BOC Edwards, Wilmington, MA, USA). Evaporations were carried out typically at base pressures lower than $2 \times 10^{-6}$ Torr. The active area of each electroluminescence (EL) device was 4 $mm^2$ and the device was characterized following a published protocol [19].

## Results and discussion

### *Synthesis of polymers*

One standard approach to synthesize PF derivatives is via the Suzuki coupling reaction using $Pd(PPh_3)_4$ to carry out the polymerization. A number of chromophores with dihalo groups have been applied to prepare PF copolymers [4]. The choice of comonomer in the fluorene-based polymer family has served as an excellent synthetic tool for designing polymers with well-balanced hole—and electron-transporting properties and fine color control. In this study, monomers **M4**, **M5** and **M6** were chosen to copolymerize with **M1** and **M2** for three PF derivatives. The feed ratio of different monomers was carefully controlled to ensure the final copolymers that would emit blue, green and red light. **M3** was then introduced to make final starlike materials. All the polymers obtained can be dissolved in common organic solvents, such as chloroform, toluene and chlorobenzene. Transparent and self-standing films can be spin-cast from their solutions.

Table 1 summarizes the composition ratio of different repeating units, molecular weights (MWs) and the molecular-weight distribution of the resulting polymers. The number-average molecular weights ($\overline{M_n}$) of these polymers range from $4.54 \times 10^3$ to $30.6 \times 10^3$, and the weight-average molecular weights ($\overline{M_w}$) range from $7.21 \times 10^3$ to $97.9 \times 10^3$. The polydispersity index ($\overline{M_w}/\overline{M_n}$) ranges from 1.58 to 3.69. The average arm numbers of the three POSS-containing polymers were calculated according to the following equation,

$$\text{Number of arms} = \left(\overline{M_n} - MW \text{ of POSS core}\right) / \left(\overline{M_n} \text{ of linear PF}\right),$$

resulting in 5.7, 3.5 and 3.1 for **POSS-P1**, **POSS-P2** and **POSS-P3**, respectively. It is certain that eight arms on POSS cannot all be replaced by polymers **P1**–**P3** owing to large steric hindrance and the random-coil nature of the polymers. The chemical structure and conformation of the final polymers were characterized by Fourier transform (FT) IR specroscopy and X-ray diffraction. Figure 1 shows the FT-IR spectra of POSS, **M3**, **P1** and **POSS-P1**. Three characteristic peaks in the POSS spectrum are found at 2250 $cm^{-1}$ (Si–H stretching), 1,256 $cm^{-1}$ (Si–$CH_3$ stretching) and 1,120 $cm^{-1}$ (Si–O–Si stretching). The disap-

*Table 2.* Thermal and optical properties of **P1**–**P3** and **POSS-P1**–**POSS-P3**

| Polymer | $T_g$ (°C) | $T_d$ (°C) | UV–vis (nm) | | | PL (nm) | | |
|---|---|---|---|---|---|---|---|---|
| | | | THF | Toluene | Film | THF | Toluene | Film |
| **P1** | 82 | 372 | 378 | 381 | 385 | 443 | 445 | 449 |
| **POSS-P1** | 110 | 413 | 375 | 378 | 380 | 441 | 442 | 449 |
| **P2** | 108 | 410 | 369 | 373 | 376 | 541 | 554 | 555 |
| **POSS-P2** | 121 | 427 | 370 | 370 | 373 | 538 | 551 | 552 |
| **P3** | 106 | 414 | 371 | 376 | 377 | 630 | 650 | 654 |
| **POSS-P3** | 128 | 428 | 371 | 375 | 377 | 631 | 651 | 652 |

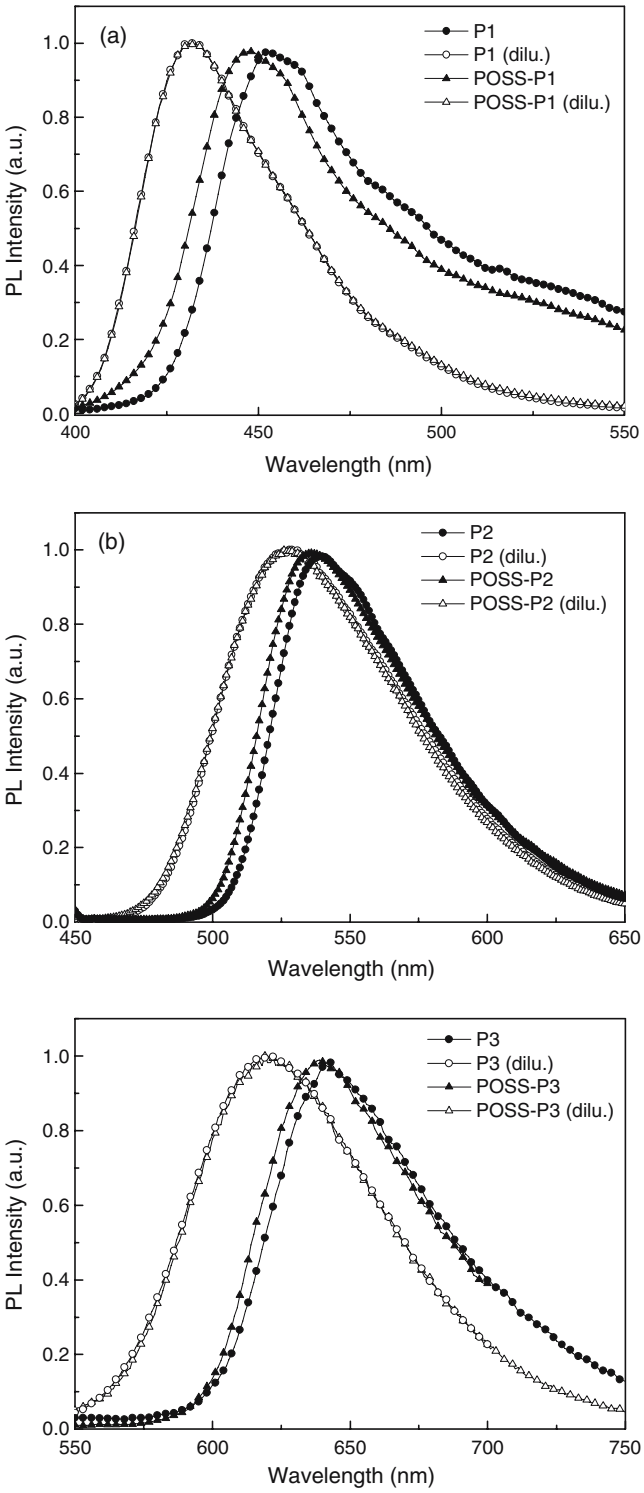


*Figure 3.* Photoluminescence (*PL*) emission spectra of **POSS-P1**–**POSS-P3** in the thin-film state.

pearance of the peak at 2,250 $cm^{-1}$ in **M3** indicates the complete attachment of 4-bromostyrene on POSS. The additional peak at 1,120 $cm^{-1}$ in **POSS-P1** is also observed as compared with **P1**, which shows the successful synthesis of the final POSS-containing material. Figure 2 shows the X-ray diffraction curves of POSS and **POSS-P1**–**POSS-P3**. The diffraction peaks of POSS are sharp owing to its well-defined structure and crystalline state. After incorporating light-emitting polymers **P1**–**P3** onto

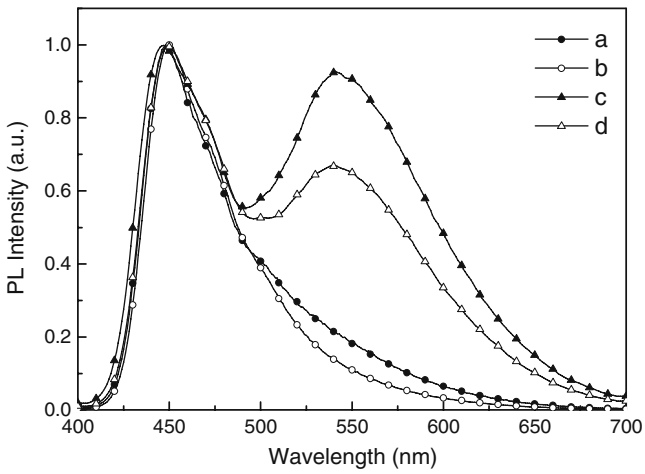


*Figure 4.* PL spectra of the annealing test of polymer thin films: (a) **P1** at 100 °C; (b) **POSS-P1** at 100 °C; (c) **P1** at 200 °C; (d) **POSS-P1** at 200 °C for 1 h each.

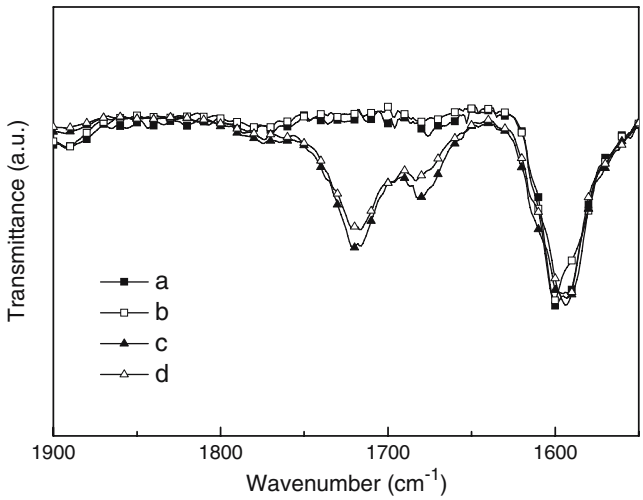


*Figure 5.* FT-IR spectra of the annealing test of polymer thin films: (a) **P1** at 100 °C; (b) **POSS-P1** at 100 °C; (c) **P1** at 200 °C; (d) **POSS-P1** at 200 °C for 1 h each.

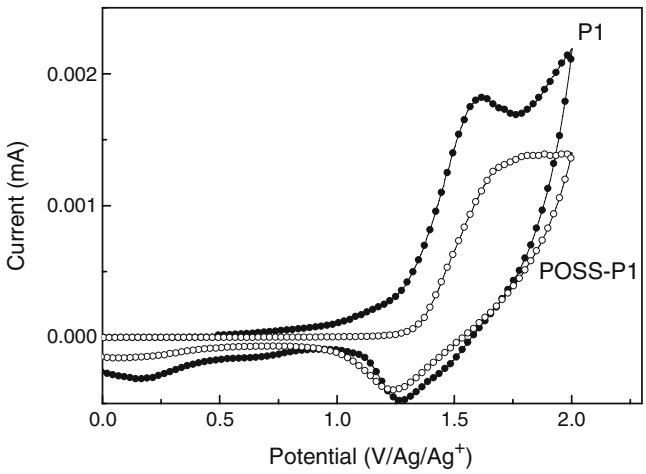


*Figure 6.* Cyclic voltammograms of **P1** and **POSS-P1**.

*Table 3.* Energy levels of **P1**–**P3** and **POSS-P1**–**POSS-P3**

| Polymer | $E_{onset}$ (V) | HOMO (eV)[a] | LUMO (eV)[b] | $E_g$ (eV)[c] |
|---|---|---|---|---|
| **P1** | 1.26 | −5.66 | −2.73 | 2.93 |
| **POSS-P1** | 1.25 | −5.65 | −2.81 | 2.84 |
| **P2** | 1.44 | −5.84 | −3.48 | 2.36 |
| **POSS-P2** | 1.37 | −5.77 | −3.34 | 2.42 |
| **P3** | 1.37 | −5.77 | −3.84 | 1.92 |
| **POSS-P3** | 1.36 | −5.76 | −3.77 | 1.99 |

[a]Estimated from the experimental equation HOMO = $-|E_{onset} + 4.4|$.
[b]Calculated from the equation $E_g$ = LUMO−HOMO.
[c]Estimated from the equation $E_g = 1.240/\lambda_{onset}$.

the POSS core, $2\theta$ became smaller and a very broad band formed at a large angle. These results indicate the amorphous state of POSS-containing materials, and the $d$ spacing of POSS increases.

### *Thermal properties*

Table 2 summarizes the thermal properties of **P1**–**P3** and **POSS-P1**–**POSS-P3**. The glass-transition temperatures ($T_g$) of **P1** and **POSS-P1** are 82 and 110 °C, respectively. The increased $T_g$ means larger confinement of polymer chains owing to the incorporation of a rigid POSS core. The thermal decomposition temperatures ($T_d$) of **P1** and **P1-POSS** are 372 and 413 °C, respectively. Similar trends were found for **POSS-P2** and **POSS-P3**, i.e., $T_g$ and $T_d$ were both enhanced after incorporating POSS into light-emitting polymers to form starlike materials. The results suggest that the incorporation of POSS enhances thermal properties and chain rigidity of linear polymers, reducing crystallinity and aggregation of chromophores in the solid state [20]. The reduction of the aggregation state was also proved by optical observation and showed benefits in light-emitting properties.

### *Optical properties*

Table 2 summarizes the UV–vis absorption and PL results of the synthesized materials in solutions and the film state. The maximum absorption bands are located in the ranges 369–378 nm in THF, 370–381 nm in toluene and 373–385 nm in the film state. It is apparent that the absorption band was not significantly changed after introducing POSS. The maximum emission bands of **POSS-P1**, **POSS-P2** and **POSS-P3** are located at 449, 552, and 652 nm, which refer to pure blue, green, and red light, respectively. The emission bands of starlike polymers are also similar to those of linear polymers. The POSS core is roughly considered to have a minor effect on the optical spectra of surrounding light-emitting polymers **P1**, **P2** or **P3**. However, some smaller changes in optical properties were noticed to deduce the reduced aggregation for those POSS-containing polymers. It is generally thought that the redshift from solution to the film state comes from the effect of interchain $\pi$-stacking, i.e., the formation of aggregates in the solid film state [21]. When the photophysical properties in two states approach each other, the extent of aggregation reduces. In Table 2, the maximum UV–vis absorption of **POSS-P1** shows a smaller difference of 5 nm in THF and the film state, as compared with its parent **P1** (approximately 7 nm). The same tendency was also observed between **POSS-P2** (approximately 3 nm) and **P2** (approximately 7 nm). The closer value of the absorption band proved the occurrence of reduced aggregation for POSS-containing PFs. The PL spectra of these polymers in concentrated and dilute solution were also obtained. Figure 3 shows the PL emission spectra of these polymers in toluene. We observed that the stellar polymers showed a smaller difference of PL emission between the two types of solutions; this helps to explain the reduced aggregation. The nonconjugated POSS is concluded to serve as an effective block to prevent aggregation and energy transfer from neighboring polymers.

The internal temperature of a light-emitting diode is known to elevate at high direct current voltage or during long-term operation. Materials with high thermal stability serve as active layers. POSS has been proven to enhance the thermal stability of light-emitting polymers. An annealing test was applied to examine the influence of

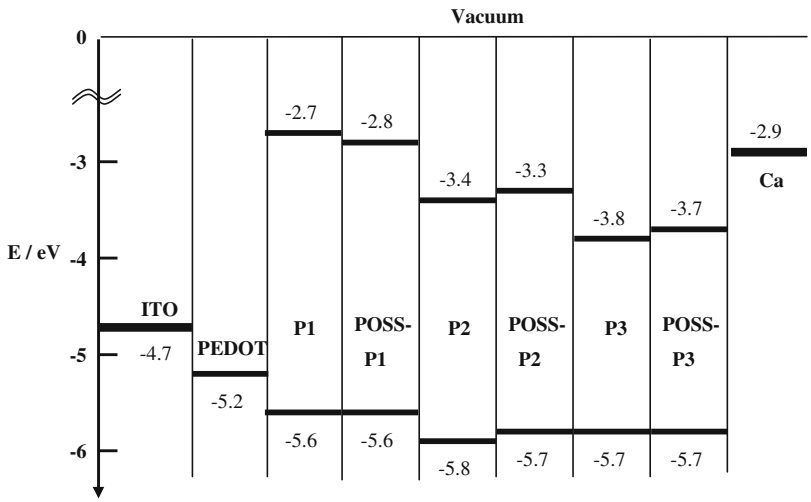


*Figure 7.* Energy-level diagram of **P1**–**P3** and **POSS-P1**–**POSS-P3**.

*Table 4.* Device performance of pristine **P1**–**P3**, **POSS-P1**–**POSS-P3** and blended polymers in indium tin oxide/poly(ethylenedioxythiophene)/polymer/Ca/Al devices

| Polymer (nm) | EL (V) | $V_{turn\text{-}on}$ | Max. brightness (cd $m^{-2}$) | Max. yield (cd $A^{-1}$) | CIE 1931 | |
|---|---|---|---|---|---|---|
| | | | | | *x* | *y* |
| **P1** | 448 | 10 | 719 | 0.27 | 0.19 | 0.21 |
| **POSS-P1** | 448 | 10 | 1.580 | 0.28 | 0.20 | 0.20 |
| **P2** | 540 | 5 | 2.568 | 0.11 | 0.39 | 0.57 |
| **POSS-P2** | 540 | 5 | 3.274 | 1.14 | 0.39 | 0.57 |
| **P3** | 656 | 7 | 642 | 0.13 | 0.68 | 0.32 |
| **POSS-P3** | 652 | 6 | 1.263 | 0.24 | 0.68 | 0.32 |
| **P1/P2** | 525 | 6 | 5.765 | 1.44 | 0.38 | 0.56 |
| **POSS-P1/POSS-P2** | 524 | 6 | 6.785 | 1.65 | 0.38 | 0.56 |
| **P1/P3** | 625 | 7 | 2.838 | 0.51 | 0.67 | 0.31 |
| **POSS-P1/POSS-P3** | 624 | 7 | 3.280 | 0.59 | 0.67 | 0.30 |

POSS on the keto defect of PFs. Figure 4 shows the PL spectra of **P1** and **POSS-P1** films after being annealed at 100 and 200 °C. The PL spectra of the annealed films at 100 °C were similar to those of fresh ones. However, a large band formed at 540 nm after annealing at 200 °C. This band is similar to the that of fluorenone formed at high temperatures or during long-term operation of devices. The newly formed band is observed both in **P1** and in **POSS-P1**, yet the intensity is smaller for **POSS-P1**. The decrease in intensity of this band indicates partial suppression of the keto defect, and the **POSS-P1** thin film becomes stabler than that of **P1**. The inhibition of fluorenone formation is further confirmed by the FT-IR spectra shown in Figure 5. The characteristic peak at 1,721 $cm^{-1}$ (carbonyl group C = O from fluorenone) formed in both **P1** and **POSS-P1** after annealing at 200 °C. The transmittance of this peak was found to be smaller in **POSS-P1**. The result is in agreement with previous reports [14, 15]. As for **POSS-P2** and **POSS-P3**, the emissive colors are green and red, respectively. The keto defect is not easily observed owing to the ease of energy transfer from a high-energy band to a low-energy band.

*Electrochemical analysis*

Cyclic voltammetry was employed to investigate the electrochemical behavior of the synthesized polymers and to estimate their energy levels. The oxidation process is clear and is directly associated with the conjugation structure of the polymer, while the reduction process is usually irreversible, poorly defined, and is associated with polymer defects or traces of impurities. Figure 6 shows cyclic voltammograms of **P1** and **POSS-P1** in the oxidation process. The HOMO energy level is determined from the onset of the oxidation curve. The energy gaps of the materials were determined from the edge of their UV–vis absorption spectra, which range from 1.92 to 2.93 eV. The energy levels of these materials are summarized in Table 3. An energy-level diagram of these materials is depicted in Figure 7.

*Device performance*

Double-layer light-emitting diodes of ITO/PEDOT/polymer/Ca/Al were fabricated to evaluate the potential of the

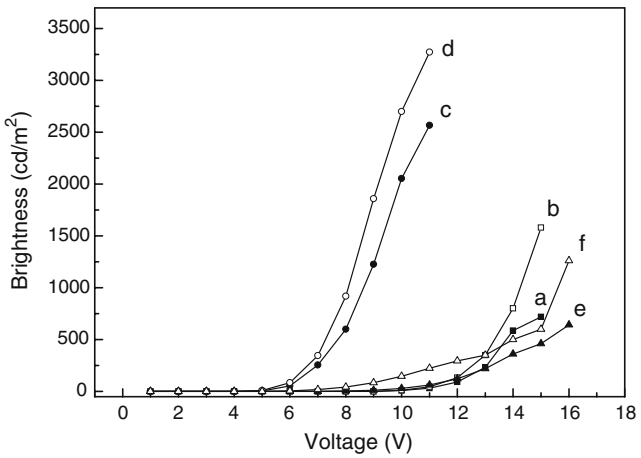


*Figure 8.* Brightness–voltage characteristics of devices using polymers as active layers: (a) **P1**; (b) **POSS-P1**; (c) **P2**; (d) **POSS-P2**; (e) **P3**; (f) **POSS-P3**.

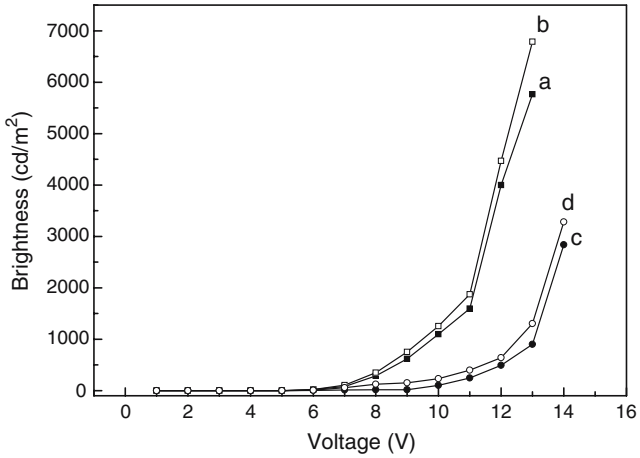


*Figure 9.* Brightness–voltage characteristics of devices using blending polymers as active layers: (a) **P1**/**P2**; (b) **POSS-P1**/**POSS-P2**; (c) **P1**/**P3**; (d) **POSS-P1**/**POSS-P3**.

synthesized materials. Device performance using these six polymers as active layers is listed in Table 4. The maximum EL bands of POSS-containing polymers are comparable to those of linear ones. Results similar to those from the PL measurements reveal that the incorporation of POSS moiety does not influence the emission properties. The turn-on voltages of those devices are also listed in Table 4. Generally speaking, the turn-on voltage is determined by some factors: film thickness and band gap of the emissive layer; injection barrier between the emissive layer and the electrode. The devices using **P1** and **POSS-P1** as active layers were observed to have the highest turn-on voltages among the six devices. Though the injection barriers of the two materials are comparatively small, the thickness and large band gap do not seem to fit the best device condition and affect the turn-on voltage. Figure 8 shows the luminescence–voltage characteristics of these devices. The maximum brightness of the **P1** device is 719 cd $m^{-2}$ with a current efficiency of 0.27 cd $A^{-1}$. With **POSS-P1** as an active layer, the maximum brightness and current efficiency were 1,580 cd $m^{-2}$ and 0.28 cd $A^{-1}$, respectively. Enhanced device performance was also observed for **POSS-P2** and **POSS-P3** compared with the corresponding linear polymers. It is suggested that the incorporation of POSS at the center core reduces aggregation of linear polymers and enhances thermal and device properties.

To further improve the performance of green—and red-light devices, the blending method was applied. The blending method has been used extensively for polymer/small molecule and organic/inorganic hybrid systems [22, 23]. Recently polymer blend diodes have been proposed and studied by Morgado et al. [24], Morteani et al. [25] and Kim et al. [26]. They found a new mechanism which allows barrier-free electron–hole capture and low-voltage, high-efficiency operation in heterojunction light-emitting diodes. In this study **P1** and **POSS-P1** were used as host matrices, while **P2**, **P3**, **POSS-P2** and **POSS-P3** were used as guest materials. The composition ratio of host-to-guest composite was chosen as 20/1 in weight percent. Figure 9 shows the luminescence–voltage characteristics of these blended devices. The maximum brightness and current efficiency using a **P1**/**P2** blend as an active layer was greatly enhanced to 5,765 cd $m^{-2}$ and 1.44 cd $A^{-1}$, respectively. The brightness was further improved to 6,785 cd $m^{-2}$ using a **POSS-P1**/**POSS-P2** blend as an active layer. Improved device performance using **P1**/**P3** or **POSS-P1**/**POSS-P3** was also obtained. The device properties of these blending materials are summarized in Table 4. The enhanced device performance is explained as follows. Firstly, the dispersion of low-band-gap materials (**P2**, **P3**, **POSS-P2** or **POSS-P3**) in the host matrix reduces aggregation and energy loss. Secondly, effective energy transfer from the host material to the guest material emits light. Thirdly, the reduction of the energy barrier between the active layer and the electrodes improves the injection and recombination of carriers. This is confirmed by the energy-level diagram of these materials in Figure 7. With **P1** or **POSS-P1** as host material, holes and electrons can be injected into the emissive layer because of the smaller energy barrier. The recombination process takes place on low-band-gap materials with emission of green or red light.

## Conclusion

Starlike materials tethered to PF derivatives emitting blue, green or red light were synthesized and characterized. POSS was incorporated into the center core of the derivatives to enhance thermal stability and reduce linear PF aggregation. The UV–vis absorption and PL emission properties of stellar polymers were similar to those of pristine ones. The keto defect was partially suppressed by POSS, which was verified by PL and FT-IR spectroscopy when the polymer films were annealed at 200 °C. Double-layer devices using POSS-containing materials as active layers showed increased performance compared with the linear PFs. Composites using **P1** or **POSS-P1** as the host matrix to blend with green—and red-light emitting PFs were created. Maximum brightness and current efficiency were further improved using the same blending materials as active layers in the double-layer electroluminescent device.

## Acknowledgments

The authors would like to thank the National Science Council of the Republic of China (NSC 93-2120-M-009-008) for financially supporting this research.

## References

1. J. H. Burroughes, D. D. C. Bradley, A. R. Brown, R. N. Marks, K. Mackay, R. H. Friend, P. L. Burn and A. B. Holmes, *Nature*, **347**, 539 (1990).
2. S. A. Chen and E. C. Chang, *Macromolecules*, **31**, 4899 (1998).
3. M. Beggren, O. Inganäs, G. Gustafsson, J. Rasmusson, M. R. Andersson, T. Hjertberg and O. Wennerström, *Nature*, **372**, 444 (1994).
4. M. T. Bernius, M. Inbasekaran, J. O'Brien and W. Wu, *Adv. Mater.*, **12**, 1737 (2000).
5. M. Woodruff, *Synth. Met.*, **80**, 257 (1996).
6. B. Liu, W. L. Yu, J. Pei, S. Y. Liu, Y. H. Lai and W. Huang, *Macromolecules*, **34**, 7932 (2001).
7. P. Herguth, X. Jiang, M. S. Liu and A. K.-Y. Jen, *Macromolecules*, **35**, 6094 (2002).
8. X. Chen, J. L. Liao, Y. Liang, M. O. Ahmed, H. E. Tseng and S. A. Chen, *J. Am. Chem. Soc.*, **125**, 636 (2003).
9. M. Grell, W. Knoll, D. Lupo, A. Meisel, T. Miteva, D. Neher, H. G. Nothofer, U. Scherf and A. Yasuda, *Adv. Mater.*, **11**, 671 (1999).
10. E. J. W. List, R. Guentner, P. Scanducci de Freitas and U. Scherf, *Adv. Mater.*, **14**, 374 (2002).
11. U. Scherf and E. J. W. List, *Adv. Mater.*, **14**, 477 (2002).
12. F. I. Wu, D. S. Reddy and C. F. Shu, *Chem. Mater.*, **15**, 269 (2003).
13. S. Xiao, M. Nguyen, X. Gong, Y. Cao, H. Wu, D. Moses and A. J. Heeger, *Adv. Funct. Mater.*, **13**, 25 (2003).
14. W. J. Lin, W. C. Chen, W. C. Wu, Y. H. Niu and A. K.-Y. Jen, *Macromolecules*, **37**, 2335 (2004).
15. C. H. Chou, S. L. Hsu, K. Dinakaran, M. Y. Chiu and K. H. Wei, *Macromolecules*, **38**, 745 (2005).
16. M. Ranger, D. Rondeau and M. Leclerc, *Macromolecules*, **30**, 7686 (1997).

17. I. S. Millard, *Synth. Met.*, **111**–**112**, 119 (2000).
18. K. Pilgram, M. Zupan and R. Sliles, *J. Heterocycl. Chem.*, **7**, 629 (1970).
19. C. H. Chen and C. W. Tang, *Appl. Phys. Lett.*, **79**, 3711 (2001).
20. S. Zheng, J. Shi and R. Mateu, *Chem. Mater.*, **12**, 1814 (2000).
21. J. H. Liao, M. Benz, E. LeGoff and M. G. Kanatzidis, *Adv. Mater.*, **6**, 135 (1994).
22. Y. Cao, I. D. Parker, G. Yu, G. Zhang and A. J. Heeger, *Nature*, **397**, 414 (1999).
23. P. W. M. Blom, H. F. M. Schoo and M. Matters, *Appl. Phys. Lett.*, **73**, 3914 (1998).
24. J. Morgado, R. H. Friend and F. Cacialli, *Appl. Phys. Lett.*, **80**, 2436 (2002).
25. A. C. Morteani, A. S. Dhoot, J. S. Kim, C. Silva, N. C. Greenham, C. E. Murphy, E. Moons, S. Ciná, J. H. Burroughes and R. H. Friend, *Adv. Mater.*, **15**, 1708 (2003).
26. J. S. Kim, P. K. H. Ho, C. E. Murphy and R. H. Friend, *Macromolecules*, **37**, 2761 (2004).